Unconditionally Stable Fundamental LOD-FDTD Method with Second-Order Temporal Accuracy and Complying Divergence

Theng Huat Gan and Eng Leong Tan, *Senior Member, IEEE,*

***Abstract*—An unconditionally stable fundamental locally one-dimensional (LOD) finite-difference time-domain (FDTD) method with second-order temporal accuracy and complying divergence (CD) (denoted as LOD2-CD-FDTD) is presented for three-dimensional (3-D) Maxwell's equations. While the conventional LOD-FDTD method does not have complying divergence, the LOD2-CD-FDTD method has complying divergence in a manner analogous to the conventional explicit FDTD method. The update procedures for a family of LOD-FDTD methods that employ similar splitting matrix operators are presented. By extending the previous concept of achieving second-order temporal accuracy for the LOD2-FDTD method via implicit output processing, we hereby propose novel, explicit output processing that not only retains second-order temporal accuracy, but also complying divergence for the LOD2-CD-FDTD method. The current source implementation for the LOD2-CD-FDTD method involves source-incorporation in only the first procedure. To further enhance efficiency, the LOD2-CD-FDTD method is formulated into the fundamental LOD2-CD-FDTD method with efficient matrix-operator-free right-hand sides. Subsequently, detailed implementation for the fundamental LOD2-CD-FDTD method is presented. Analytical proof is provided to ascertain the second-order temporal accuracy of the LOD2-CD-FDTD method. Numerical results and examples are also presented to validate the divergence-complying property of the LOD2-CD-FDTD method.**

***Index Terms*—Finite-difference time-domain (FDTD), locally one-dimensional (LOD), alternating-direction-implicit (ADI), unconditionally stable methods, Maxwell's equations, divergence.**

I. Introduction

TIME-domain electromagnetic techniques allow one to visualize the interaction of the electromagnetic waves with the physical environment. The conventional explicit finite-difference time-domain (FDTD) method is a widely used numerical technique for such analysis, as it implements the Maxwell's equations in a straightforward and systematic approach [1]. The Maxwell's equations depicts four physical laws: the Faraday's law and Ampere's law are expressed using the curl operator, while the Gauss's laws for the electric and magnetic fields are expressed using the divergence operator.

The conventional explicit FDTD method employs second-order central-difference in time and space to solve the curl equations. Due to the manner in which the field components are structured in the Yee's cell and the spatial-differencing operations of the scheme, the conventional explicit FDTD method inherently enforces the Gauss's laws for the electric and magnetic fields [2]. Hence, the conventional explicit FDTD method complies with the full set of Maxwell's equations, and is a true three-dimensional (3-D) Maxwell's solver.

However, the conventional FDTD method is an explicit method that is only conditionally stable. The time step size is restricted by the Courant-Fredrich-Lewy (CFL) stability criterion. As such, the computed results may grow without bound when time-marching proceeds with the CFL limit violated. To eliminate such a constraint, unconditionally stable implicit FDTD methods were proposed. The most popular one being the alternating-direction-implicit finite-difference time-domain (ADI-FDTD) method [3], [4]. The conventional ADI-FDTD method has two procedures where the field components are updated implicitly in alternating direction for both procedures.

Another class of unconditionally stable implicit FDTD method is the locally one-dimensional finite-difference time-domain (LOD-FDTD) method [5], [6]. Similar to the conventional ADI-FDTD method, the conventional LOD-FDTD method is a two-procedure method with implicit field updating for both procedures. Moreover, each procedure is effectively reduced to a one-dimensional update equation locally. Therefore, the conventional LOD-FDTD method is more computationally efficient. While the conventional ADI-FDTD method is second-order temporal accurate, the conventional LOD-FDTD method has only first-order temporal accuracy.

The above mentioned unconditionally stable implicit FDTD methods have been recently simplified into the fundamental schemes [7]–[9]. The fundamental schemes of the ADI-FDTD and LOD-FDTD methods are more efficient and simpler to implement, even though they are equivalent to the conventional methods and share similar numerical properties.

While the conventional explicit FDTD method has complying divergence, the conventional ADI-FDTD method does not have complying divergence [10], [11] as the Maxwell's curl equations are being enforced based on locally inconsistent scheme. Although the conventional ADI-FDTD method uses the same Yee's cell as the conventional explicit FDTD method, the spatial-differencing operations of the former method do not inherently enforce the Gauss's laws for the electric and magnetic fields. Recently, the conventional ADI-FDTD method has been reformulated into the more efficient leapfrog ADI-FDTD method. However, the analysis of the divergence properties of the leapfrog ADI-FDTD method shows that this variant of the

Theng Huat Gan is with DSO National Laboratories, Singapore 118230 (e-mail: gthenghu@dso.org.sg).

Eng Leong Tan is with the School of Electrical and Electronics Engineering, Nanyang Technological University, Singapore 639798 (e-mail: eeltan@ntu.edu.sg).

Manuscript received .

T. H. Gan and E. L. Tan, "Unconditionally Stable Fundamental LOD-FDTD Method with Second-Order Temporal Accuracy and Complying Divergence," IEEE Transactions on Antennas and Propagation, Vol. 61, No. 5, pp. 2630-2638, May 2013. DOI: 10.1109/TAP.2013.2242036

ADI-FDTD method still does not have complying divergence [12]. Similarly, the conventional LOD-FDTD method, which we will discuss at length in the subsequent sections, also does not have complying divergence. Spurious charges may exist in the source-free regions when the method is not divergence-complying. Consequently, there would be additional grid capacitance in such regions.

In this paper, we present the unconditionally stable fundamental locally one-dimensional finite-difference time-domain method with second-order temporal accuracy and complying divergence (denoted as LOD2-CD-FDTD) for 3-D Maxwell's equations. Section II presents the update procedures for a family of LOD-FDTD methods that employ similar splitting matrix operators. Section III extends the previous concept of achieving second-order temporal accuracy for the LOD2-FDTD method via implicit output processing, and propose a novel, explicit output processing that not only retains second-order temporal accuracy, but also complying divergence for the LOD2-CD-FDTD method. The current source implementation for the LOD2-CD-FDTD method involves source-incorporation in only the first procedure. To further enhance efficiency, the LOD2-CD-FDTD method is formulated into the fundamental LOD2-CD-FDTD method with efficient matrix-operator-free right-hand side (RHS). Subsequently, detailed implementation for the fundamental LOD2-CD-FDTD method will be presented. Analytical proof for the second-order temporal accuracy of the LOD2-CD-FDTD method is provided. In Section IV, numerical results and examples will be presented to validate the divergence-complying property of the LOD2-CD-FDTD method.

II. Family of LOD-FDTD Methods

In this section, we present a family of LOD-FDTD methods for 3-D Maxwell's equations in a medium with permittivity ϵ and permeability μ. In this family, we select the splitting matrix operators of Maxwell's equations as follows:

$$\mathbf{A} = \begin{pmatrix} 0 & 0 & 0 & 0 & 0 & \frac{1}{\epsilon}\partial_y \\ 0 & 0 & 0 & \frac{1}{\epsilon}\partial_z & 0 & 0 \\ 0 & 0 & 0 & 0 & \frac{1}{\epsilon}\partial_x & 0 \\ 0 & \frac{1}{\mu}\partial_z & 0 & 0 & 0 & 0 \\ 0 & 0 & \frac{1}{\mu}\partial_x & 0 & 0 & 0 \\ \frac{1}{\mu}\partial_y & 0 & 0 & 0 & 0 & 0 \end{pmatrix} \tag{1a}$$

$$\mathbf{B} = \begin{pmatrix} 0 & 0 & 0 & 0 & \frac{-1}{\epsilon}\partial_z & 0 \\ 0 & 0 & 0 & 0 & 0 & \frac{-1}{\epsilon}\partial_x \\ 0 & 0 & 0 & \frac{-1}{\epsilon}\partial_y & 0 & 0 \\ 0 & 0 & \frac{-1}{\mu}\partial_y & 0 & 0 & 0 \\ \frac{-1}{\mu}\partial_z & 0 & 0 & 0 & 0 & 0 \\ 0 & \frac{-1}{\mu}\partial_x & 0 & 0 & 0 & 0 \end{pmatrix} \tag{1b}$$

where ∂_x, ∂_y, ∂_z are the spatial difference operators for the first derivatives along x, y, z directions, respectively.

A. LOD1-FDTD Method

The conventional LOD1-FDTD method comprises two updating procedures in the main iterations:

$$\left(\mathbf{I} - \frac{\Delta t}{2}\mathbf{A}\right) \mathbf{u}_{\text{LOD1}}^{n+\frac{1}{2}} = \left(\mathbf{I} + \frac{\Delta t}{2}\mathbf{A}\right) \mathbf{u}_{\text{LOD1}}^{n} \tag{2a}$$

$$\left(\mathbf{I} - \frac{\Delta t}{2}\mathbf{B}\right) \mathbf{u}_{\text{LOD1}}^{n+1} = \left(\mathbf{I} + \frac{\Delta t}{2}\mathbf{B}\right) \mathbf{u}_{\text{LOD1}}^{n+\frac{1}{2}} \tag{2b}$$

where

$$\mathbf{u} = \begin{bmatrix} E_x & E_y & E_z & H_x & H_y & H_z \end{bmatrix}^T \tag{3}$$

and $\mathbf{I}$ is the 6 x 6 identity matrix. The subscript "LOD1" denotes the first-order temporal accurate LOD-FDTD method. It is noted that the field components for the conventional LOD1-FDTD method are only updated in one direction for each procedure. This allows for a more efficient implementation and is useful especially in parallel processing [13].

B. LOD2-FDTD Method

The conventional LOD1-FDTD method above is only of first-order temporal accuracy [14] as the matrix operators $\mathbf{A}$ and $\mathbf{B}$ do not commute. In order to achieve second-order temporal accuracy, the LOD2-FDTD method which retains the two-procedure updating scheme of the conventional LOD1-FDTD method, but with shift in time indices was proposed as [6]

$$\left(\mathbf{I} - \frac{\Delta t}{2}\mathbf{A}\right) \mathbf{u}^{n+\frac{3}{4}} = \left(\mathbf{I} + \frac{\Delta t}{2}\mathbf{A}\right) \mathbf{u}^{n+\frac{1}{4}} \tag{4a}$$

$$\left(\mathbf{I} - \frac{\Delta t}{2}\mathbf{B}\right) \mathbf{u}^{n+1\frac{1}{4}} = \left(\mathbf{I} + \frac{\Delta t}{2}\mathbf{B}\right) \mathbf{u}^{n+\frac{3}{4}} \tag{4b}$$

In addition, input processing for initial fields $\mathbf{u}^{t=0}$ may be performed at time step $n = 0$ as

$$\left(\mathbf{I} - \frac{\Delta t}{4}\mathbf{B}\right) \mathbf{u}^{\frac{1}{4}} = \left(\mathbf{I} + \frac{\Delta t}{4}\mathbf{B}\right) \mathbf{u}^{t=0} \tag{5}$$

and output processing at time step $n + 1$ reads

$$\left(\mathbf{I} + \frac{\Delta t}{4}\mathbf{B}\right) \mathbf{u}_{\text{LOD2}}^{n+1} = \left(\mathbf{I} - \frac{\Delta t}{4}\mathbf{B}\right) \mathbf{u}^{n+1\frac{1}{4}} \tag{6}$$

The subscript "LOD2" denotes the second-order temporal accurate LOD-FDTD method.

The input processing is to be invoked only once at the beginning and may often be omitted for electromagnetic excitation problems with null initial fields. The output processing can be performed separately and in parallel — independent of the main iterations. Furthermore, the output field components are usually required at only certain desired observation points and time instants. Hence, the output processing is to be invoked only when necessary. Note that (5) and (6) are implicit input and output processing.

It is worth mentioning that although the split-step approach may also achieve second-order temporal accuracy, it requires three updating procedures at every time step [15], [16]. The LOD2-FDTD method only requires two updating procedures with output processing to be invoked only when necessary.

III. LOD2-FDTD WITH COMPLYING DIVERGENCE

By extending the previous concept of achieving second-order temporal accuracy for the LOD2-FDTD method via implicit output processing, we hereby propose novel, explicit output processing that not only retains second-order temporal accuracy, but also complying divergence for the LOD2-CD-FDTD method. We have

$$\left(\mathbf{I}-\frac{\Delta t}{2}\mathbf{A}\right)\,\mathbf{u}^{n+\frac{1}{2}}=\left(\mathbf{I}+\frac{\Delta t}{2}\mathbf{A}\right)\,\mathbf{u}^{n}+\Delta t\,\mathbf{s}^{n+\frac{1}{2}} \tag{7a}$$

$$\left(\mathbf{I}-\frac{\Delta t}{2}\mathbf{B}\right)\,\mathbf{u}^{n+1}=\left(\mathbf{I}+\frac{\Delta t}{2}\mathbf{B}\right)\,\mathbf{u}^{n+\frac{1}{2}} \tag{7b}$$

where

$$\mathbf{s}=\left[\tfrac{-1}{\epsilon}J_x\quad \tfrac{-1}{\epsilon}J_y\quad \tfrac{-1}{\epsilon}J_z\quad \tfrac{-1}{\mu}M_x\quad \tfrac{-1}{\mu}M_y\quad \tfrac{-1}{\mu}M_z\right]^T \tag{8}$$

for the main iterations. For null initial fields, $\mathbf{u}^{n+1}=\mathbf{u}^{n+1}_{\text{LOD1}}$ and $\mathbf{u}^{n+\frac{1}{2}}=\mathbf{u}^{n+\frac{1}{2}}_{\text{LOD1}}$. On the other hand, for nonzero initial fields $\mathbf{u}^{t=0}$, implicit input processing needs to be invoked (only once) at time step $n=0$ as

$$\left(\mathbf{I}-\frac{\Delta t}{2}\mathbf{B}\right)\,\mathbf{u}^{0}=\mathbf{u}^{t=0} \tag{9}$$

The explicit output processing at time step $n+1$ is

$$\mathbf{u}^{n+1}_{\text{CD}}=\left(\mathbf{I}-\frac{\Delta t}{2}\mathbf{B}\right)\,\mathbf{u}^{n+1} \tag{10}$$

where the subscript "CD" denotes complying divergence.

The update equations for the main iterations of the LOD2-CD-FDTD method in (7) are simply those of the conventional LOD1-FDTD method. Furthermore, the current implementation of the LOD2-CD-FDTD method involves source-incorporation in the first procedure only, similar to the concise current source implementation [17]. It is also worthwhile to mention that $\mathbf{u}^{n+1}_{\text{CD}}$ is the final field output from the explicit output processing (10), while $\mathbf{u}^{n+1}$ is the field variable for the main iterations.

A. Fundamental LOD2-CD-FDTD Method

To further enhance efficiency, we formulate the LOD2-CD-FDTD method into the fundamental form (denoted as FLOD2-CD-FDTD), with its right-hand sides free of matrix operators **A** and **B**, by introducing auxiliary variable

$$\mathbf{v}=\left[e_x\quad e_y\quad e_z\quad h_x\quad h_y\quad h_z\right]^T \tag{11}$$

We manipulate (7) to yield (cf. [7] for more details) :

$$\left(\frac{1}{2}\mathbf{I}-\frac{\Delta t}{4}\mathbf{A}\right)\,\mathbf{v}^{n+\frac{1}{2}}=\mathbf{u}^{n}+\frac{\Delta t}{2}\mathbf{s}^{n+\frac{1}{2}} \tag{12a}$$

$$\mathbf{u}^{n+\frac{1}{2}}=\mathbf{v}^{n+\frac{1}{2}}-\mathbf{u}^{n} \tag{12b}$$

$$\left(\frac{1}{2}\mathbf{I}-\frac{\Delta t}{4}\mathbf{B}\right)\,\mathbf{v}^{n+1}=\mathbf{u}^{n+\frac{1}{2}} \tag{12c}$$

$$\mathbf{u}^{n+1}=\mathbf{v}^{n+1}-\mathbf{u}^{n+\frac{1}{2}} \tag{12d}$$

Notice that the RHS of (12) are all matrix-free as compared to (7). This results in substantial reduction of floating point operations (flops) count and memory indexing. Furthermore, (9) is already in the fundamental implicit form (matrix-operator free RHS), while (10) is already in the fundamental explicit form (matrix-operator free LHS). Therefore, no further simplification is required for these equations.

B. Implementation of FLOD2-CD-FDTD Method

We now present the actual implementation of the FLOD2-CD-FDTD method in detail. For additional savings of operations and memory, we have omitted the auxiliary fields h's by absorbing them into the physical fields H's. The main iterations comprise two updating procedures as follows

First substep from n to $n+\frac{1}{2}$:

1) Auxiliary (implicit) updating for $e^{n+\frac{1}{2}}$

$$\frac{1}{2}e_x^{n+\frac{1}{2}}-\frac{\Delta t^2}{8\mu\epsilon}\partial_y^2\,e_x^{n+\frac{1}{2}}=E_x^n+\frac{\Delta t}{2\epsilon}\partial_y\,H_z^n -\frac{\Delta t}{2\epsilon}J_x^{n+\frac{1}{2}}-\frac{\Delta t^2}{4\mu\epsilon}\partial_y\,M_z^{n+\frac{1}{2}} \tag{13a}$$

$$\frac{1}{2}e_y^{n+\frac{1}{2}}-\frac{\Delta t^2}{8\mu\epsilon}\partial_z^2\,e_y^{n+\frac{1}{2}}=E_y^n+\frac{\Delta t}{2\epsilon}\partial_z\,H_x^n -\frac{\Delta t}{2\epsilon}J_y^{n+\frac{1}{2}}-\frac{\Delta t^2}{4\mu\epsilon}\partial_z\,M_x^{n+\frac{1}{2}} \tag{13b}$$

$$\frac{1}{2}e_z^{n+\frac{1}{2}}-\frac{\Delta t^2}{8\mu\epsilon}\partial_x^2\,e_z^{n+\frac{1}{2}}=E_z^n+\frac{\Delta t}{2\epsilon}\partial_x\,H_y^n -\frac{\Delta t}{2\epsilon}J_z^{n+\frac{1}{2}}-\frac{\Delta t^2}{4\mu\epsilon}\partial_x\,M_y^{n+\frac{1}{2}} \tag{13c}$$

2) Explicit updating for $E^{n+\frac{1}{2}}$

$$E_\xi^{n+\frac{1}{2}}=e_\xi^{n+\frac{1}{2}}-E_\xi^n,\ \ \xi=x,\ y,\ z \tag{14}$$

3) Explicit updating for for $H^{n+\frac{1}{2}}$

$$H_x^{n+\frac{1}{2}}=H_x^n+\frac{\Delta t}{2\mu}\partial_z\,e_y^{n+\frac{1}{2}}-\frac{\Delta t}{\mu}M_x^{n+\frac{1}{2}} \tag{15a}$$

$$H_y^{n+\frac{1}{2}}=H_y^n+\frac{\Delta t}{2\mu}\partial_x\,e_z^{n+\frac{1}{2}}-\frac{\Delta t}{\mu}M_y^{n+\frac{1}{2}} \tag{15b}$$

$$H_z^{n+\frac{1}{2}}=H_z^n+\frac{\Delta t}{2\mu}\partial_y\,e_x^{n+\frac{1}{2}}-\frac{\Delta t}{\mu}M_z^{n+\frac{1}{2}} \tag{15c}$$

Second substep from $n+\frac{1}{2}$ to $n+1$:

1) Auxiliary (implicit) updating for e^{n+1}

$$\frac{1}{2}e_x^{n+1}-\frac{\Delta t^2}{8\mu\epsilon}\partial_z^2\ e_x^{n+1}=E_x^{n+\frac{1}{2}}-\frac{\Delta t}{2\epsilon}\partial_z\ H_y^{n+\frac{1}{2}} \tag{16a}$$

$$\frac{1}{2}e_y^{n+1}-\frac{\Delta t^2}{8\mu\epsilon}\partial_x^2\ e_y^{n+1}=E_y^{n+\frac{1}{2}}-\frac{\Delta t}{2\epsilon}\partial_x\ H_z^{n+\frac{1}{2}} \tag{16b}$$

$$\frac{1}{2}e_z^{n+1}-\frac{\Delta t^2}{8\mu\epsilon}\partial_y^2\ e_z^{n+1}=E_z^{n+\frac{1}{2}}-\frac{\Delta t}{2\epsilon}\partial_y\ H_x^{n+\frac{1}{2}} \tag{16c}$$

2) Explicit updating for E^{n+1}

$$E_\xi^{n+1}=e_\xi^{n+1}-E_\xi^{n+\frac{1}{2}},\ \ \xi=x,\ y,\ z \tag{17}$$

3) Explicit updating for H^{n+1}

$$H_x^{n+1}=H_x^{n+\frac{1}{2}}-\frac{\Delta t}{2\mu}\partial_y\ e_z^{n+1} \tag{18a}$$

$$H_y^{n+1}=H_y^{n+\frac{1}{2}}-\frac{\Delta t}{2\mu}\partial_z\ e_x^{n+1} \tag{18b}$$

$$H_z^{n+1}=H_z^{n+\frac{1}{2}}-\frac{\Delta t}{2\mu}\partial_x\ e_y^{n+1} \tag{18c}$$

Input processing at $n=0$ (only for nonzero initial fields $E^{t=0}$ and $H^{t=0}$) :

1) Implicit updating for E^0

$$E_x^0-\frac{\Delta t^2}{4\mu\epsilon}\partial_z^2\ E_x^0=E_x^{t=0}-\frac{\Delta t}{2\epsilon}\partial_z\ H_y^{t=0} \tag{19a}$$

$$E_y^0-\frac{\Delta t^2}{4\mu\epsilon}\partial_x^2\ E_y^0=E_y^{t=0}-\frac{\Delta t}{2\epsilon}\partial_x\ H_z^{t=0} \tag{19b}$$

$$E_z^0-\frac{\Delta t^2}{4\mu\epsilon}\partial_y^2\ E_z^0=E_z^{t=0}-\frac{\Delta t}{2\epsilon}\partial_y\ H_x^{t=0} \tag{19c}$$

2) Explicit updating for H^0

$$H_x^0=H_x^{t=0}-\frac{\Delta t}{2\mu}\partial_y\ E_z^0 \tag{20a}$$

$$H_y^0=H_y^{t=0}-\frac{\Delta t}{2\mu}\partial_z\ E_x^0 \tag{20b}$$

$$H_z^0=H_z^{t=0}-\frac{\Delta t}{2\mu}\partial_x\ E_y^0 \tag{20c}$$

Output processing at $n+1$ (only whenever and wherever necessary) :

1) Explicit updating for E_{CD}^{n+1}

$$E_{x_{\text{CD}}}^{n+1}=E_x^{n+1}+\frac{\Delta t}{2\epsilon}\partial_z\ H_y^{n+1} \tag{21a}$$

$$E_{y_{\text{CD}}}^{n+1}=E_y^{n+1}+\frac{\Delta t}{2\epsilon}\partial_x\ H_z^{n+1} \tag{21b}$$

$$E_{z_{\text{CD}}}^{n+1}=E_z^{n+1}+\frac{\Delta t}{2\epsilon}\partial_y\ H_x^{n+1} \tag{21c}$$

2) Explicit updating for H_{CD}^{n+1}

$$H_{x_{\text{CD}}}^{n+1}=H_x^{n+1}+\frac{\Delta t}{2\mu}\partial_y\ E_z^{n+1} \tag{22a}$$

$$H_{y_{\text{CD}}}^{n+1}=H_y^{n+1}+\frac{\Delta t}{2\mu}\partial_z\ E_x^{n+1} \tag{22b}$$

$$H_{z_{\text{CD}}}^{n+1}=H_z^{n+1}+\frac{\Delta t}{2\mu}\partial_x\ E_y^{n+1} \tag{22c}$$

As mentioned previously, the input processing is to be invoked only once at the beginning and may often be omitted for null initial fields, while the output processing may be performed independent of the main iterations at only some specific observation locations when field data are required.

It is interesting to note that the output processing of the LOD2-CD-FDTD method consists only of explicit update equations, and does not require a tridiagonal solution that is necessary for the LOD2-FDTD method. Therefore, the output processing for the former is in general more efficient.

C. Temporal Order of LOD2-CD-FDTD Method

Next, we proceed to determine the temporal order of the LOD2-CD-FDTD method. The main iterations of the LOD2-CD-FDTD method comprise the LOD1-FDTD update equations with n iterations, i.e.

$$\begin{aligned}\mathbf{G}_{\text{LOD1}}^n\ &=\Big[\Big(\mathbf{I}-\tfrac{\Delta t}{2}\mathbf{B}\Big)^{-1}\Big(\mathbf{I}+\tfrac{\Delta t}{2}\mathbf{B}\Big)\Big(\mathbf{I}-\tfrac{\Delta t}{2}\mathbf{A}\Big)^{-1}\\&\qquad\cdot\Big(\mathbf{I}+\tfrac{\Delta t}{2}\mathbf{A}\Big)\Big]^n\end{aligned} \tag{23}$$

where $\mathbf{G}_{\text{LOD1}}$ is the amplification matrix of the LOD1-FDTD method. Subsequently (23) can be expanded as

$$\begin{aligned}&\mathbf{G}_{\text{LOD1}}^n=\mathbf{I}+n\Delta t\Big(\mathbf{A}+\mathbf{B}\Big)\\&+\Big(\frac{n\Delta t^2}{2}\Big)\Big[n\mathbf{A}^2+\Big(n-1\Big)\mathbf{AB}+\Big(n+1\Big)\mathbf{BA}+n\mathbf{B}^2\Big]\\&\qquad+O\Big(\Delta t^3\Big)\end{aligned} \tag{24}$$

which shows only the first-order temporal accuracy. Next, we perform input processing and some manipulation as

$$\begin{aligned}&\mathbf{G}_{\text{LOD1}}^n\Big(\mathbf{I}-\frac{\Delta t}{2}\mathbf{B}\Big)^{-1}=\mathbf{I}+\Delta t\Big[n\mathbf{A}+\Big(n+\frac{1}{2}\Big)\mathbf{B}\Big]\\&+\frac{\Delta t^2}{2}\Big[n^2\mathbf{A}^2+n^2\mathbf{AB}+\Big(n^2+n\Big)\mathbf{BA}\\&\quad+\Big(n^2+n+\frac{1}{2}\Big)\mathbf{B}^2\Big]+O\Big(\Delta t^3\Big)\end{aligned} \tag{25}$$

TABLE I
COMPARISON OF MAIN FEATURES OF VARIOUS FDTD METHODS.

Method	Unconditionally Stable	Complexity	Total (RHS) M/D + A/S	Field Array	Temporal Order	Complying Divergence
Conventional explicit FDTD	No	Low	30	6	2^{nd}	Yes
ADI-FDTD	Yes	Moderate High	102	9	2^{nd}	No
LOD1-FDTD	Yes	Moderate Low	72	9	1^{st}	No
LOD2-FDTD	Yes	Moderate Low	72	9	2^{nd}	No
Fundamental LOD2-CD-FDTD	Yes	Low	42	9	2^{nd}	Yes

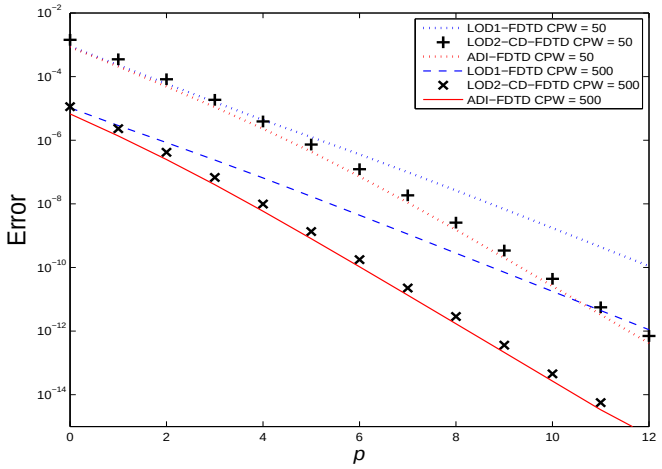

Fig. 1. Normalized norm errors vs. p of geometric time subdivision ($\Delta t = \Delta t_{CFL}/2^p$) for the LOD2-CD-FDTD, LOD1-FDTD method and ADI-FDTD method.

Finally by performing output processing, we can obtain the amplification matrix of the LOD2-CD-FDTD method

$$\mathbf{G}_{\text{CD}}^n = \Big(\mathbf{I} - \frac{\Delta t}{2}\mathbf{B}\Big)\mathbf{G}_{\text{LOD1}}^n\Big(\mathbf{I} - \frac{\Delta t}{2}\mathbf{B}\Big)^{-1} \tag{26a}$$

$$= \mathbf{I} + n\Delta t\Big(\mathbf{A} + \mathbf{B}\Big) + \frac{n^2\Delta t^2}{2}\Big(\mathbf{A}^2 + \mathbf{AB} + \mathbf{BA} + \mathbf{B}^2\Big) + O\Big(\Delta t^3\Big) \tag{26b}$$

Equation (26b) agrees with the analytical solution of $e^{(\mathbf{A}+\mathbf{B})\Delta t}$ throughout the Δt^2 terms. Thus, the LOD2-CD-FDTD method is accurate to second-order in time.

To show the temporal order of the LOD2-CD-FDTD method numerically, we chose the cells per freespace wavelength (CPW) as 50 and 500 at 3 GHz. Fig. 1 plots the normalized norm errors vs. p of geometric time subdivision ($\Delta t = \Delta t_{CFL}/2^p$) for the LOD2-CD-FDTD method and LOD1-FDTD method. The Courant limit time step size is $\Delta t_{CFL} = \frac{\Delta}{c\sqrt{3}}$, where c is the speed of light in freespace. It can be seen that the norm errors of the LOD2-CD-FDTD method decrease with second order, while the norm errors of the LOD1-FDTD method decrease with first order.

The LOD2-CD-FDTD method is an improved extension of the LOD1-FDTD method, which is an unconditionally stable FDTD method since the magnitudes of the eigenvalues of $\mathbf{G}_{\text{LOD1}}$ are unity. The input and output processing of the LOD2-CD-FDTD method perform simple additional arithmetic operations that are never iterated in the main iterations, and as such will not cause the field components to grow without bound. Indeed from (26a), $(\mathbf{I} - \frac{\Delta t}{2}\mathbf{B})$ and its inverse are not raised to n. It is also interesting to note that $\mathbf{G}_{\text{CD}}^n$ and $\mathbf{G}_{\text{LOD1}}^n$ are related simply by similarity transformation. Thus, the LOD2-CD-FDTD method will also be unconditionally stable in an analogous manner to the LOD1-FDTD method. The stability condition of the LOD2-CD-FDTD method is the same as the LOD1-FDTD method.

Table I presents the comparison of the main features of the conventional explicit FDTD method, ADI-FDTD method, LOD1-FDTD method, LOD2-FDTD method and FLOD2-CD-FDTD method. It is clear that the FLOD2-CD-FDTD method has most of the main features of the conventional explicit FDTD method while being unconditionally stable. In addition, the table also includes the total flops count for multiplications/divisions (M/D) and additions/subtractions (A/S) required for one complete time step of various FDTD methods. Among the unconditionally stable FDTD methods, it is apparent that the FLOD2-CD-FDTD method has the least flops count. This flops reduction is due to the fundamental form of the FLOD2-CD-FDTD method, with its RHS free of matrix operators. Furthermore, the memory requirement of the FLOD2-CD-FDTD method is still the same as the ADI-FDTD method and LOD1-FDTD method. Note that the flops count does not include the computation cost of solving the tridiagonal matrix. Detailed discussion for the above may be found in [7].

IV. NUMERICAL RESULTS

In this section, we present numerical results to compare and validate the divergence-complying property of the LOD2-CD-FDTD method for 3-D Maxwell's equations. The Gauss's law for the electric field in differential form states that

$$\nabla \cdot \mathbf{D} = \nabla \cdot \epsilon\,\mathbf{E} = \rho_v \tag{27}$$

where $\mathbf{D}$ is the electric flux density and ρ_v is the volume charge density.

In the absence of charge, (27) states that the divergence of the electric flux density is zero. To examine the divergence of

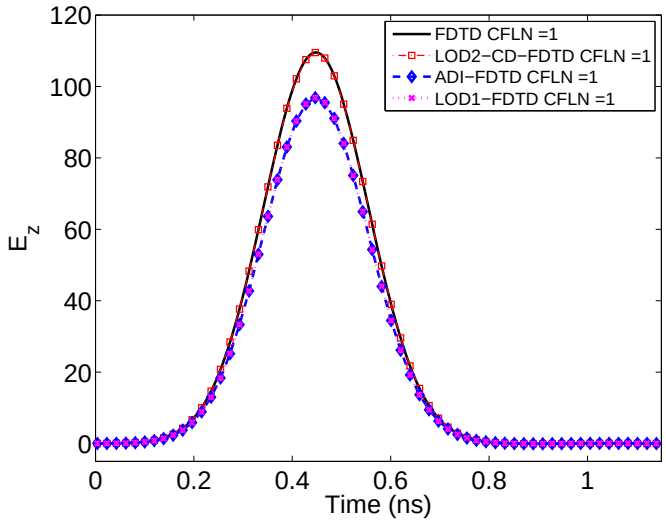

Fig. 2. Time-domain E_z field component computed using conventional explicit FDTD, LOD2-CD-FDTD, ADI-FDTD and LOD1-FDTD for CFLN = 1. Good agreement is shown between the LOD2-CD-FDTD method and the conventional explicit FDTD method.

electric flux density, we employ the finite-difference method to (27) as

$$\nabla \cdot \epsilon \, \mathbf{E} = \partial_x\big(\epsilon E_x\big) + \partial_y\big(\epsilon E_y\big) + \partial_z\big(\epsilon E_z\big). \tag{28}$$

A. Numerical Validation

To validate the divergence-complying property of the LOD2-CD-FDTD method, we simulate an air-filled perfect electric conductor (PEC) cavity meshed with 50 x 30 x 9 uniform cell of size 2 mm each. A point source excited by a differentiated Gaussian pulse is located at the center of the cavity as

$$J_z = \frac{t - t_0}{\tau} \; e^{-\left(\frac{t-t_0}{\tau}\right)^2} \tag{29}$$

where

$$\tau = 150 \text{ ps}, \; t_0 = 3\tau.$$

The divergence of electric flux density is computed numerically using (28), and converted to a decibel scale referenced to 1 Coulomb per meter cube (C/m^3) as

$$\nabla \cdot \widehat{\mathbf{D}} \text{ (dB)} = 10 \; \log_{10}\left(\frac{\nabla \cdot \mathbf{D}}{1 \text{ C/m}^3}\right). \tag{30}$$

We compare the divergence of $\widehat{\mathbf{D}}$ for the LOD2-CD-FDTD method, conventional explicit FDTD method, ADI-FDTD method and LOD1-FDTD method. The Courant limit time step size is $\Delta t_{CFL} = \frac{\Delta}{c\sqrt{3}}$ where c is the speed of light in freespace. We also denote CFLN $= \frac{\Delta t}{\Delta t_{CFL}}$.

Fig. 2 graphs the time-domain E_z field component computed using the conventional explicit FDTD method, LOD2-CD-FDTD method, ADI-FDTD method and LOD1-FDTD method for CFLN = 1. Here, the output processing is performed at only one location (observation point) for all time steps as

$$E_{z_{\text{CD}}}|^{n+1}_{25,15,5\frac{1}{2}} = E_z|^{n+1}_{25,15,5\frac{1}{2}} + \frac{\Delta t}{2\epsilon\Delta y}\left(H_x|^{n+1}_{25,15\frac{1}{2},5\frac{1}{2}} - H_x|^{n+1}_{25,14\frac{1}{2},5\frac{1}{2}}\right) \tag{31}$$

Good agreement is shown between the LOD2-CD-FDTD method and the conventional explicit FDTD method. However, the E_z field component of the ADI-FDTD method and the LOD1-FDTD method differs from the conventional explicit FDTD and LOD2-CD-FDTD method.

During the source excitation period, the E_z field component is around its peak value at time t = 0.446 ns, while at time t = 1.232 ns the source excitation has already died off. Henceforth, we shall sample the electric fields at time t = 0.446 ns to investigate the divergence of $\widehat{\mathbf{D}}$ in the presence of a source. Likewise, to investigate the divergence of $\widehat{\mathbf{D}}$ in the absence of a source, we sample the electric fields at time t = 1.232 ns. As discussed previously, the presence of a source would indicate the existence of a corresponding charge density.

Fig. 3 shows the divergence of $\widehat{\mathbf{D}}$ for the conventional explicit FDTD method, LOD2-CD-FDTD method, ADI-FDTD method and LOD1-FDTD method in the grid regions around the source point for CFLN = 1 at time t = 0.446 ns. The divergence of $\widehat{\mathbf{D}}$ is plotted in the xy-plane at k = 5. The peak in the middle of the grid indicates the source excitation location, while the rest of the grids are the source-free regions. Here, the output processing is performed at only one time step (observation time instant) in the xy-plane at k = 5 and is given by

$$E_{z_{\text{CD}}}|^{n+1=116}_{i,j,5\frac{1}{2}} = E_z|^{n+1=116}_{i,j,5\frac{1}{2}} + \frac{\Delta t}{2\epsilon\Delta y}\left(H_x|^{n+1=116}_{i,j+\frac{1}{2},5\frac{1}{2}} - H_x|^{n+1=116}_{i,j-\frac{1}{2},5\frac{1}{2}}\right) \tag{32}$$

Referring to Fig. 3, it is clear that the LOD2-CD-FDTD method has similar divergence-complying property as the conventional explicit FDTD method. At the source excitation location, the divergence of $\widehat{\mathbf{D}}$ for both LOD2-CD-FDTD and conventional explicit FDTD methods is approximately -58 dB, while at the source-free regions, the divergence of $\widehat{\mathbf{D}}$ is about -250 dB. Such level of divergence of $\widehat{\mathbf{D}}$ for the source-free regions is good enough subjected to numerical noise floor.

On the other hand, the divergence of $\widehat{\mathbf{D}}$ for the ADI-FDTD method and the LOD1-FDTD method is significantly higher than the conventional explicit FDTD method and the LOD2-CD-FDTD method in the source-free regions. Thus, it is evident that the LOD2-CD-FDTD method has complying divergence, while the ADI-FDTD and LOD1-FDTD methods do not have complying divergence.

It is of interest to ascertain the divergence-complying property of the LOD2-CD-FDTD method at higher CFLN. To that end, we chose CFLN = 8 and exclude the conventional explicit FDTD method (as it is unstable for CFLN $>$ 1). Fig. 4 shows

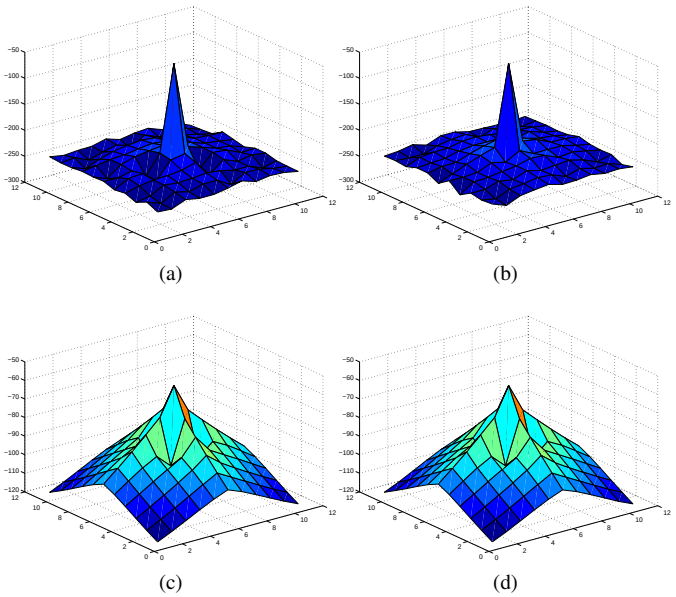

Fig. 3. Divergence of $\widehat{\mathbf{D}}$ for CFLN = 1 at time t = 0.446 ns (presence of source excitation). (a) Conventional explicit FDTD. (b) LOD2-CD-FDTD. (c) ADI-FDTD. (d) LOD1-FDTD. The divergence of $\widehat{\mathbf{D}}$ for the LOD2-CD-FDTD method agrees well with the conventional explicit FDTD method.

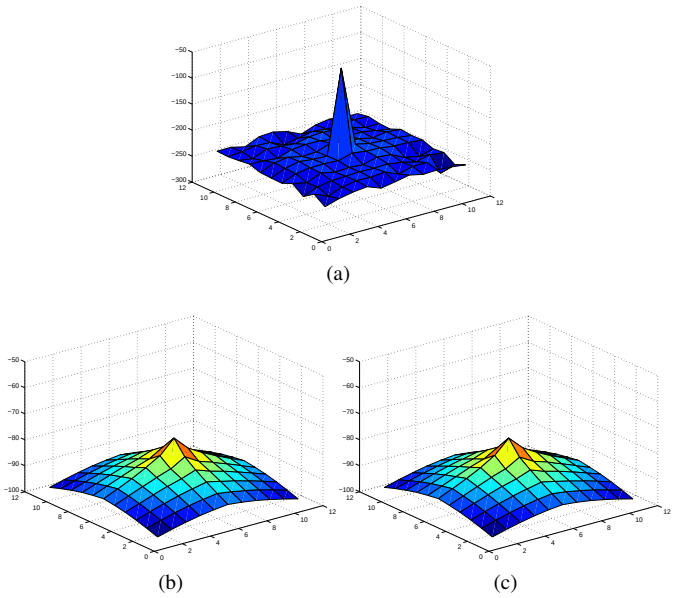

Fig. 4. Divergence of $\widehat{\mathbf{D}}$ for CFLN = 8 at time t = 0.446 ns (presence of source excitation) (a) LOD2-CD-FDTD. (b) ADI-FDTD. (c) LOD1-FDTD. The divergence-complying property of the LOD2-CD-FDTD method is still evident even at higher CFLN.

the snapshot of the divergence of $\widehat{\mathbf{D}}$ for the LOD2-CD-FDTD method, ADI-FDTD method and LOD1-FDTD method in the grid regions around the source for CFLN = 8 at time t = 0.446 ns. The divergence-complying property of the LOD2-CD-FDTD method is still evident even at higher CFLN. However, the divergence of $\widehat{\mathbf{D}}$ for the ADI-FDTD and LOD1-FDTD methods increases slightly at the source-free regions for CFLN = 8.

Next, we illustrate the divergence-complying property of the LOD2-CD-FDTD method in the absence of source for CFLN = 8. Fig. 5 presents the snapshot of the divergence of $\widehat{\mathbf{D}}$ for the LOD2-CD-FDTD method, ADI-FDTD method and LOD1-FDTD method in the grid regions around the source point for CFLN = 8 at time t = 1.232 ns.

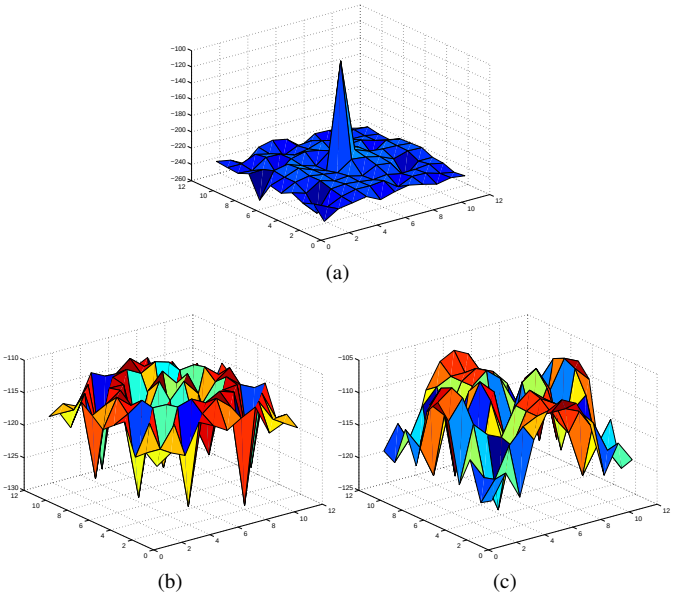

Fig. 5. Divergence of $\widehat{\mathbf{D}}$ for CFLN = 8 at time t = 1.232 ns (absence of source excitation) (a) LOD2-CD-FDTD. (b) ADI-FDTD. (c) LOD1-FDTD.

Referring to Fig. 5(a), it can be observed that the divergence-complying property of the LOD2-CD-FDTD method remains the same even when the source excitation has died off. At the source excitation location, the divergence of $\widehat{\mathbf{D}}$ for the LOD2-CD-FDTD method is approximately -104 dB. This static charge is deposited onto the Yee's cell by the source excitation and remains in the grid. Although it is not shown here, the conventional explicit FDTD method (for CFLN $\leq$ 1) also displays similar phenomenon [18].

Upon comparing Figs. 5(b) and 5(c), we note that the divergence of $\widehat{\mathbf{D}}$ for the ADI-FDTD method is lower than the LOD1-FDTD method. For such methods, spurious charges exist even in the source-free regions. These spurious charges may affect the accuracy of simulations especially for problems involving capacitances or passive lumped elements [19].

B. Divergence Analysis

In this subsection, we present further analysis of the divergence property to compare the divergence of electric field for the LOD2-CD-FDTD method, conventional explicit FDTD method, ADI-FDTD method and LOD1-FDTD method. For brevity, details of the analysis have been omitted but may be found in [12].

Fig. 6 plots the divergence of $\widehat{E}_0$ (dB) vs. propagation angle ϕ for the conventional explicit FDTD method, LOD2-CD-FDTD method, ADI-FDTD method and LOD1-FDTD method for CFLN = 1 and CPW = 20. Here, propagation angles θ and ϕ are defined using the spherical coordinate system (θ = elevation angle and ϕ = azimuthal angle). From the figures, it can be observed that the ADI-FDTD method and LOD1-FDTD method are not divergence-free in the source-free regions.

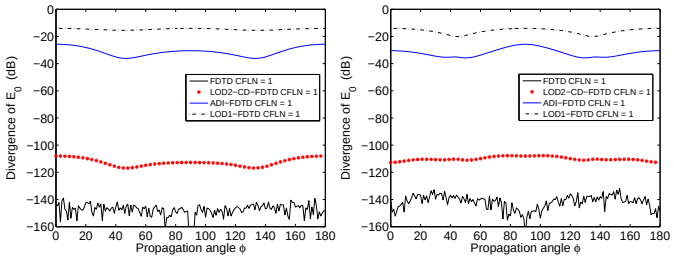

(a) (b)

Fig. 6. Divergence of $\widehat{E}_0$ (dB) vs. propagation angle ϕ for the conventional explicit FDTD, LOD2-CD-FDTD, ADI-FDTD and LOD1-FDTD method for CFLN = 1 and CPW = 20. (a) $\theta = 30°$ (b) $\theta = 60°$ (θ = elevation angle and ϕ = azimuthal angle).

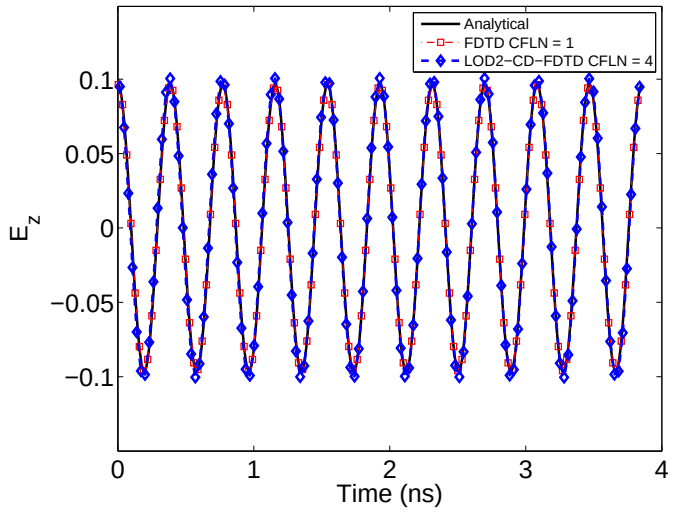

Fig. 7. Time-domain E_z field component computed using the analytical method, conventional explicit FDTD method and LOD2-CD-FDTD method

On the other hand, the divergence of $\widehat{E}_0$ for the LOD2-CD-FDTD method is much lower than the ADI-FDTD method and LOD1-FDTD method. From the divergence analysis as well as numerical validation in the previous subsection, we have shown that the LOD2-CD-FDTD method is divergence-complying in a manner analogous to the conventional explicit FDTD method.

C. Accuracy and Efficiency

To demonstrate the accuracy of the LOD2-CD-FDTD method, we simulate an air-filled cavity meshed with 50 x 50 x 50 uniform cells of size 2 mm each. It is initialized with TE_{111}-mode fields at time t = 0 and the observation point is located at cell (31,31,26). Fig. 7 depicts the time-domain E_z field component computed using the analytical method, conventional explicit FDTD method and LOD2-CD-FDTD method. The CFLN for the conventional explicit FDTD method is 1, while the CFLN for the LOD2-CD-FDTD method is 4. The LOD2-CD-FDTD method agrees well with the analytical solution of the TE_{111}-mode fields.

Next, we compare the efficiency of various FDTD methods based on the CPU time taken to simulate a cavity of

TABLE II
CPU TIME (SECONDS) OF VARIOUS FDTD METHODS.

Method	CFLN 1	CFLN 4
Conventional explicit FDTD	1738	-
ADI-FDTD	6049	1520
LOD1-FDTD	5127	1289
Fundamental LOD2-CD-FDTD	4278	1067

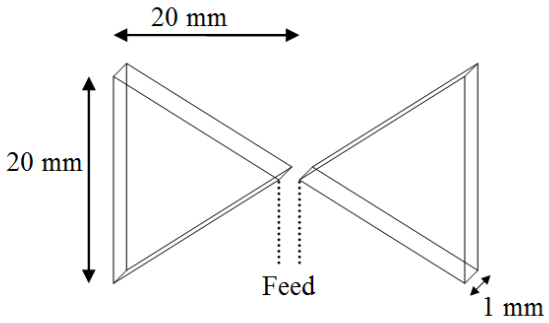

Fig. 8. Configuration of bow-tie antenna.

100 x 100 x 100 uniform cells. The simulations are terminated at the same time instant $t = \frac{20000\ \Delta t_{CFL}}{\text{CFLN}}$. The CFLN is chosen as 1 and 4. Hence, the number of iterations are 20000 and 5000, respectively. The programs have been compiled using Microsoft Visual C++ under Microsoft Win7 (32-Bit) operating system, and run on a platform of 3.1 GHz Intel I5 processor with 4 GB RAM.

Table II compares the CPU time (seconds) taken by the conventional explicit FDTD method, ADI-FDTD method, LOD1-FDTD method and FLOD2-CD-FDTD method. As expected, the unconditionally stable FDTD methods require more CPU time than the conventional explicit FDTD method for CFLN = 1. However for CFLN = 4, the FLOD2-CD-FDTD method requires 38.6% less time than the conventional explicit FDTD method, and 17.2% less time than the LOD1-FDTD method.

V. NUMERICAL EXAMPLE

In this example, we simulate a bow-tie antenna which may be useful for the detection of breast cancer [20]. The computation domain consists of 100 x 100 x 50 uniform cells with size $\Delta = \Delta_x = \Delta_y = \Delta_z = 1$ mm. It is terminated by a 10 cell perfectly matched layer absorbing boundary condition.

Fig. 8 illustrates the configuration of the bow-tie antenna. It is fed at its apex with a sinusoidal modulated Gaussian pulse excitation given by

$$J_x = \sin\left[2\pi f_0\Big(t - t_0\Big)\right] e^{-\left(\frac{t-t_0}{\tau}\right)^2} \tag{33}$$

where

$$f_0 = 2 \text{ GHz},\ \tau = 150 \text{ ps},\ t_0 = 3\tau.$$

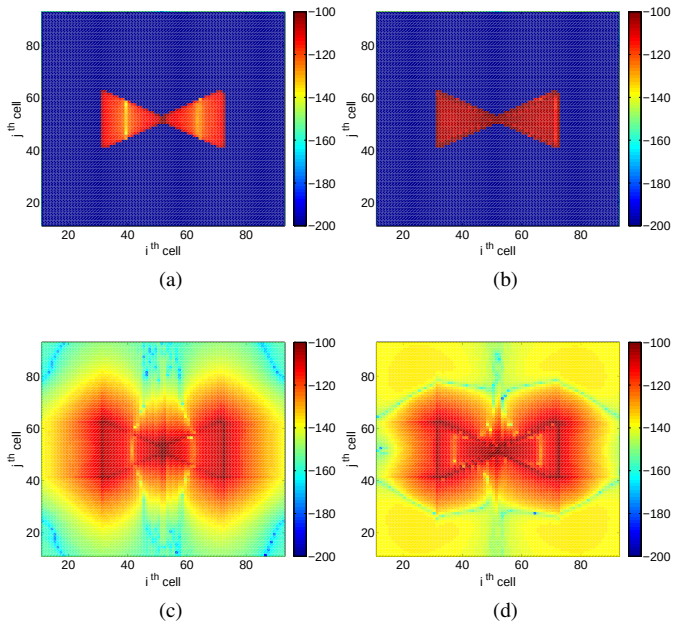

Fig. 9. Divergence of $\widehat{\mathbf{D}}$ for the bow-tie antenna at time t = 0.962 ns. (a) Conventional explicit FDTD with CFLN = 1. (b) LOD2-CD-FDTD with CFLN = 8. (c) ADI-FDTD with CFLN = 8. (d) LOD1-FDTD with CFLN = 8. The geometry of the bow-tie antenna can be clearly seen for both conventional explicit FDTD and LOD2-CD-FDTD methods.

The CFLN for the conventional explicit FDTD method is 1, while the CFLN for the implicit FDTD methods is 8. Fig. 9 compares the divergence of $\widehat{\mathbf{D}}$ for the bow-tie antenna at time t = 0.962 ns for the conventional explicit FDTD method, LOD2-CD-FDTD method, ADI-FDTD method and LOD1-FDTD method. It can be observed from the figure that charges are only deposited onto the surface of the bow-tie antenna for the LOD2-CD-FDTD method and the conventional explicit FDTD method. Moreover, it is interesting to note that the geometry of the bow-tie antenna can be clearly seen.

However, significant amount of charge can still be found in the source-free regions surrounding the bow-tie antenna for the ADI-FDTD method and LOD1-FDTD method. It is not clear where the boundaries of the bow-tie antenna are, as the charges on the bow-tie antenna are almost the same as the surrounding source-free regions.

For the conventional explicit FDTD method and LOD2-CD-FDTD method, the divergence of $\widehat{\mathbf{D}}$ in freespace is about 100 dB lower than the divergence of $\widehat{\mathbf{D}}$ on the surface of the bow-tie antenna. On the other hand, for the ADI-FDTD method and LOD1-FDTD method, the divergence of $\widehat{\mathbf{D}}$ in freespace about 20 cells away from the boundary of the bow-tie antenna is only 20 dB lower than the divergence of $\widehat{\mathbf{D}}$ on the surface of the bow-tie antenna.

VI. Conclusion

This paper has presented an unconditionally stable fundamental LOD2-CD-FDTD method with second-order temporal accuracy and complying divergence for 3-D Maxwell's equations. The update procedures for a family of LOD-FDTD methods that employ similar splitting matrix operators have been presented. By extending the previous concept of achieving second-order temporal accuracy for the LOD2-FDTD method via implicit output processing, we have proposed a novel, explicit output processing that not only retains second-order temporal accuracy, but also complying divergence for the LOD2-CD-FDTD method. The output processing of the LOD2-CD-FDTD method consists only of explicit update equations, and does not require a tridiagonal solution that is necessary for the LOD2-FDTD method. The current source implementation for the LOD2-CD-FDTD method involves source-incorporation in only the first procedure. To further enhance efficiency, the LOD2-CD-FDTD method has been formulated into the fundamental LOD2-CD-FDTD method with efficient matrix-operator-free right-hand side. In addition, detailed implementation of the fundamental LOD2-CD-FDTD method has been presented. Analytical proof has been provided for the second-order temporal accuracy of the LOD2-CD-FDTD method. Numerical results and examples have been presented to validate the divergence-complying property of the LOD2-CD-FDTD method.

The LOD2-CD-FDTD method has complying divergence, and thus complies with Maxwell's equations. It does not have spurious charge in the source-free regions, and consequently would not incur any additional grid capacitance.

References

[1] K. S. Yee, "Numerical solution of initial boundary value problems involving Maxwell's equations in isotropic media," *IEEE Trans. Antennas Propagat.*, vol. 14, no. 3, pp. 302-307, May 1966.

[2] A. Taflove and S. C. Hagness, *Computational Electrodynamics: The Finite-Difference Time-Domain Method, 3rd ed.*, Boston, M. A: Artech House, 2005.

[3] T. Namiki, "3-D ADI-FDTD method - Unconditionally stable time-domain algorithm for solving full vector Maxwells equations," *IEEE Trans. Microw. Theory Tech.*, vol. 48, no. 10, pp. 1743-1748, Oct. 2000.

[4] F. Zheng, Z. Chen, and J. Zhang, "Toward the development of a three-dimensional unconditionally stable finite-difference time-domain method," *IEEE Trans. Microw. Theory Tech.*, vol. 48, no. 9, pp. 1550-1558, Sept. 2000.

[5] W. Fu. and E. L. Tan, "Development of split-step FDTD method with higher-order spatial accuracy," *Electron. Lett.*, vol. 40, no. 20, pp. 1252-1254, Sep. 2004.

[6] E. L. Tan, "Unconditionally stable LOD-FDTD method for 3-D Maxwell's equations, " *IEEE Microw. Wireless Comp. Lett.*, vol. 17, no. 2, pp. 85-87, Feb. 2007.

[7] E. L. Tan, "Fundamental schemes for efficient unconditionally stable implicit finite-difference time-domain methods," *IEEE Trans. Antennas Propagat.*, vol. 56, no. 1, pp. 170-177, Jan. 2008.

[8] J. Shibayama, T. Oikawa, J. Yamauchi and H. Nakano,"Efficient LOD-BOR-FDTD implementation based on a fundamental scheme ,"*IEEE Photon. Technol. Lett*, vol. 48, no. 13, Apr. 2012.

[9] J. Shibayama, T. Hirano, J. Yamauchi and H. Nakano,"Efficient implementation of frequency-dependent 3D LOD-FDTD method using fundamental scheme ,"*Electron. Lett.*, Jun. 2012.

[10] S. G. Garcia, R. G. Rubio, A. R. Bretones and R. G. Martin, "On the dispersion relation of ADI-FDTD," *IEEE Microw. Wireless Comp. Lett.*, vol. 16, no. 6, pp. 354-356, Jun. 2006.

[11] K. Y. Jung, F. L. Teixeira, S. G. Garcia and R. Lee, "On numerical artifacts of the complex envelope ADI-FDTD method," *IEEE Trans. Antennas Propagat.*, vol. 57, no. 2, pp. 491-498, Feb. 2009.

[12] T. H. Gan and E. L. Tan, "Analysis of the divergence properties for the three-dimensional leapfrog ADI-FDTD method," *IEEE Trans. Antennas Propagat.*, vol. 60, no. 12, pp. 5801-5808, Dec. 2012.

[13] E. L. Tan, "Acceleration of LOD-FDTD method using fundamental scheme on graphics processor units," *IEEE Microw. Wireless Comp. Lett.*, vol. 20, no. 12, pp. 648-650, Dec. 2010.

[14] Q. F. Liu, Z. Chen and W. Y. Yin, "An arbitrary-order LOD-FDTD method and its stability and numerical dispersion," *IEEE Trans. Antennas Propagat.*, vol. 57, no. 8, pp. 2409-2417, Aug. 2009.
[15] J. Lee and B. Fornberg, "A split-step approach for the 3-D Maxwell's equations," *J. Comput. Appl. Math.*, vol. 158, pp. 485-505, 2003.
[16] J. Lee and B. Fornberg, "Some unconditionally stable time stepping methods for the 3-D Maxwell's equations," *J. Comput. Appl. Math.*, vol. 166, pp. 497-523, 2004.
[17] E. L. Tan, "Concise current source implementation for efficient 3-D ADI-FDTD method", *IEEE Microw. Wireless Comp. Lett.*, vol. 17, no. 11, pp. 748-750, Nov. 2007.
[18] C. L. Wagner and J. B. Schneider, "Divergent fields, charge, and capacitance in FDTD simulations," *IEEE Trans. Antennas Propagat.*, vol. 46, no. 12, pp. 2131-2136, 1998.
[19] W. Fu. and E. L. Tan, "Unconditionally stable ADI-FDTD method including passive lumped elements," *IEEE Trans. Electromagn. Compat.*, vol. 48, no. 4, pp. 661-668, Nov. 2006.
[20] S. C. Hagness, A. Taflove and J. E. Bridges, "Three-dimensional FDTD analysis of a pulsed microwave confocal system for breast cancer detection: design of an antenna-array element," *IEEE Trans. Antennas Propagat.*, vol. 47, no. 5, pp. 783-791, May 1999.

Theng Huat Gan (S'10) received the B.Eng. (Electrical) degree with first class honors from Nanyang Technological University, Singapore, in 2007.

Currently, he is a Member of Technical Staff at the DSO National Laboratories. His research interest includes antenna design and computational electromagnetics.

Mr Gan received the DSO postgraduate scholarship award. He was awarded the Defence Technology Price team award (Singapore) in 2009 and 2010.

Eng Leong Tan (SM'06) received the B.Eng. (Electrical) degree with first class honors from the University of Malaya, Malaysia, and the Ph.D. degree in Electrical Engineering from Nanyang Technological University, Singapore.

From 1991 to 1992, he was a Research Assistant at the University of Malaya. From 1991 to 1994, he worked part time at Commercial Network Corporations Sdn. Bhd., Malaysia. From 1999 to 2002, he was a Member of Technical Staff at the Institute for Infocomm Research, Singapore. Since 2002, he has been with the School of Electrical & Electronic Engineering, Nanyang Technological University, where he is currently an Associate Professor. His research interests include computational electromagnetics and acoustics, RF/microwave circuit and antenna design.